Molecular Dynamics in Linear and Multiarmed Star Polymers of *cis*-Polyisoprene As Studied by Dielectric Spectroscopy

Diethelm Boese,*,† Friedrich Kremer,† and Lewis J. Fetters‡

Max-Planck-Institut für Polymerforschung, Postfach 3148, 6500 Mainz, FRG, and Exxon Research and Engineering Company, Corporate Research Laboratories, Route 22E, Annandale, New Jersey 08801. *Received July 1, 1989; Revised Manuscript Received October 7, 1989*

ABSTRACT: Dielectric spectroscopy from 10^{-1} to 10^{9} Hz was used to investigate bulk amorphous multiarmed stars of *cis*-polyisoprene and their linear counterparts, both having narrow molecular weight distributions. The star polymers resemble the linear polymers in showing two distinct regions of dielectric dispersion. A molecular weight independent segmental process occurs at nearly the same frequency as in the linear polymer due to dipole moments perpendicular to the chain backbone. The second process is caused by the parallel dipole moments and exhibits a pronounced molecular weight dependence. The relaxation time of the molecular weight dependent normal-mode process for linear polymers can be described according to the Rouse theory below the critical molecular weight, M_c ($\cong 10^4$), but above M_c it corresponds to the 3.7 power of M_w, which is characteristic for entangled macromolecules. A similar dependence of the relaxation time is observed for the many armed star polymers. It is interpreted by means of the conformational scaling properties of Daoud and Cotton and compared with theoretical and computational approaches.

I. Introduction

Star-branched polymers with arms of equal length allow an investigation of the influence of the topological structure on molecular dynamics. In our recent study[1] we presented dielectric relaxation experiments on bulk linear *cis*-polyisoprene and 8-arm stars of polyisoprene, both having approximately the same molecular weight or arm molecular weight. Linear polymers as well as star-branched polymers of *cis*-isoprene show two distinct regions of dielectric dispersion. Due to the lack of symmetry in its chemical structure *cis*-polyisoprene has nonzero components of the dipole moment both perpendicular and parallel to the chain contour. Thus, two dielectric relaxation processes, a segmental- and normal-mode process, are present.[2–6] The latter is caused by the parallel dipole components while the segmental-mode process has its origin in local motions of the perpendicular dipole components.

Experimental studies of the dielectric relaxation in star-branched molecules were started by Stockmayer and Burke.[7,8] These authors found that the dielectric relaxation time of the normal-mode process in poly(propylene oxide) can be predicted from the molecular weight and the bulk viscosity, using the theoretical models of Ham[9] or Zimm and Kilb.[10] Furthermore, they compared the dielectric relaxation times of linear chains with those of star-branched polymers. Adachi and Kotaka[11] discussed the degree of branching in solutions of linear poly(2,6-dichloro-1,4-phenylene oxide) and its influence on the dielectric relaxation times.

In the present article the dielectric relaxation properties of entangled bulk amorphous 3-, 4-, 8-, 12-, and 18-arm polyisoprene stars are compared with those of the linear polyisoprenes. The relaxation behavior of the star polymers is interpreted with the conformational scaling properties predicted by Daoud and Cotton[12] and compared with theoretical and computational approaches.[13–15]

† Max-Planck-Institut für Polymerforschung.
‡ Exxon Research and Engineering Co.

Table I
Characteristics of Linear Polyisoprene

				microstructure content, %		
sample[a]	$10^{-3}M_w$	M_w/M_n	T_g,[b] K	cis-1,4	trans-1,4	vinyl-3,4
PIP-01	1.1		200.0	74.6	18.4	7.0
PIP-05	5.1	1.03	207.1	78.8	17.9	3.3
PIP-08	8.4	1.03	211.2	78.8	16.2	5.0
PIP-13	13.1	1.03	211.5	77.9	18.1	4.0
PIP-17	17.2	1.02	213.1	76.4	17.8	5.8
PIP-38	38.2	1.03	213.1	78.6	16.7	4.7
PIP-65	65.0	1.03	213.2	78.5	16.7	4.8
PIP-97	97.0	1.02	213.2	75.7	18.1	6.2

[a] Nomenclature: PIP-05, e.g., corresponds to polyisoprene of molecular weight 5 kg mol^{-1}. [b] Extrapolation of the DSC data[18] to the 0° heating rate limit yields an asymptotic T_g value of −205 K for this type of polyisoprene.

II. Experimental Section

Preparation and characterization of the 3-, 4-, 8-, 12-, and 18-arm polyisoprene stars were performed by using the methods described elsewhere.[16–20] Linear *cis*-polyisoprene was prepared by anionic polymerization in hexane at 303 K with *sec*-butyllithium as initiator to produce linear polymers with narrow molecular weight distributions. Weight-average molecular weights (M_w) of the stars and the star arms (M_{arm}) were determined by light scattering and in some cases, for the arms, by osmotic pressure. Size-exclusion chromatography (SEC) was used to monitor the removal (via fractionation) of unlinked arms from the stars. For the linear *cis*-polyisoprene weight-average molecular weights were determined by low-angle light scattering and osmometry while SEC was used to determine the molecular weight distribution (M_w/M_n). The microstructure of linear and starshaped *cis*-polyisoprene was analyzed using ^{13}C NMR.[21] The glass transition temperature, T_g, was determined from DSC at a heating rate of 20 K/min. The results are listed in Tables I and II.

The dielectric measurements covered the frequency range from 10^{-1} to 10^{9} Hz. Three different measurement systems were used: (1) A Solartron–Schlumberger frequency response analyzer FRA 1254, which was supplemented by using a high-impedance preamplifier of variable gain,[22] covered the frequency range from 10^{-4} to 6×10^{4} Hz. (2) In the audiofrequency range of 10–10^{7} Hz a Hewlett-Packard impedance analyzer 4192A was used. For both parts the sample material was kept between two condenser plates (gold-plated stainless steel electrodes; diameter

0024-9297/90/2223-1826$02.50/0

Table II
Characteristics of Multiarmed Polyisoprene Stars

sample[a]	$10^{-4}M_w$ (star)	$10^{-3}M_a$ (arm)	T_g, K	microstructure content, %		
				cis-1,4	trans-1,4	vinyl-3,4
SPIP-3-11	3.5	11.4	213.0	78.6	16.1	5.3
SPIP-4-15	6.1	15.3	213.4	77.6	16.7	5.7
SPIP-4-30	12.2	30.5	212.2	77.6	16.8	5.6
SPIP-4-44	17.3	44.0	213.8	78.9	16.1	5.0
SPIP-4-95	38.0	95.0	213.5	77.9	16.7	5.6
SPIP-8-05	4.0	5.0	212.3	76.3	17.8	5.9
SPIP-8-08	6.0	7.5	213.6	75.4	18.5	6.1
SPIP-8-14	11.0	13.8	211.9	77.3	17.7	5.0
SPIP-8-16	12.4	15.5	213.4	80.4	15.5	4.1
SPIP-8-100	79.5	99.4	214.0	77.9	16.6	5.5
SPIP-12-03	4.1	3.4	211.7	79.1	16.6	4.3
SPIP-12-08	9.6	8.0	211.9	79.6	16.0	4.4
SPIP-12-21	25.0	20.8	212.9	80.5	15.6	3.9
SPIP-12-68	81.0	67.5	213.5	77.2	17.0	5.8
SPIP-18-03	6.4	3.5	213.1	77.4	17.4	5.2
SPIP-18-11	19.7	10.9	213.7	76.2	18.0	5.8
SPIP-18-12	21.8	12.1	212.9	77.5	17.5	5.0
SPIP-18-21	38.4	21.3	213.0	76.5	17.9	5.6
SPIP-18-44	80.0	44.4	212.5	77.2	17.2	5.6

[a] Nomenclature: SPIP-8-05, e.g., corresponds to a star polyisoprene with eight arms and an arm molecular weight of 5 kg mol^{-1}.

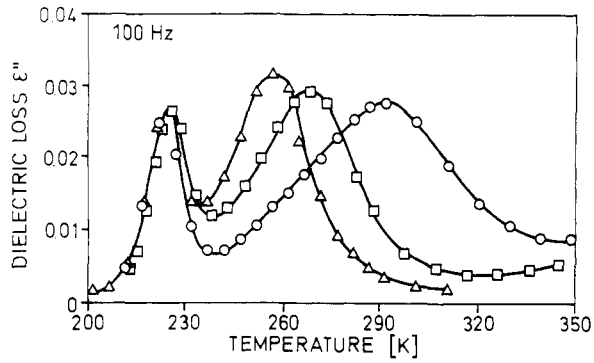

Figure 1. Temperature dependence of the dielectric loss, ϵ'', at 100 Hz for the 8-arm polyisoprene star of different molecular weights (see Table II): △, SPIP-8-05; □, SPIP-8-08; ○, SPIP-8-14.

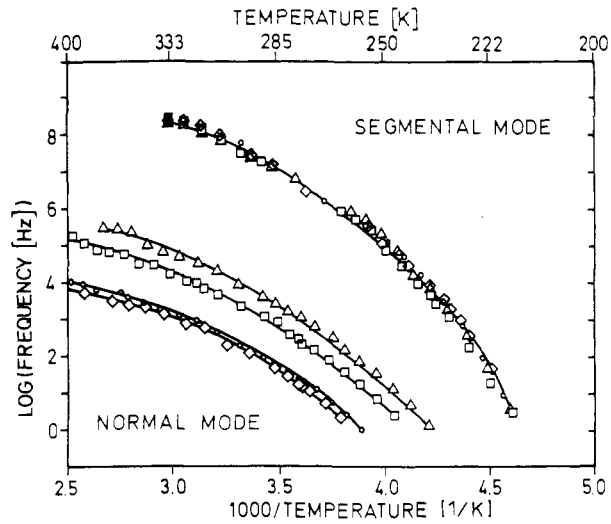

Figure 2. Activation plot for the segmental mode and normal mode of the 8-arm polyisoprene star: △, SPIP-8-05; □, SPIP-8-08; ○, SPIP-8-14; ◇, SPIP-8-16.

40 mm). (3) For measurements between 10^6 and 10^9 Hz a Hewlett-Packard impedance analyzer 4191A was employed, which is based on the principle of a reflectometer. A small sample condenser (diameter 6 mm) was mounted as a part of the inner conductor of a coaxial cell. All three arrangements were placed in custom-made cryostats wherein the sample was placed in a stream of temperature-controlled nitrogen gas, which allowed temperature adjustment from 100 K up to 500 K with ±0.02 K.[1,6]

III. Results

As reported previously[1] undiluted 8-arm polyisoprene stars show two distinct regions of dielectric dispersion. The two processes are well separated on the frequency and temperature scale; the initial process occurs around 215 K while the secondary one appears above 240 K (Figures 1 and 2). The temperature and frequency dependence of the dielectric loss $\epsilon''(\nu)$ for bulk SPIP-18-11 is shown in Figure 3. It also reveals a low-temperature event around 215 K, which has its origin in local motions of the perpendicular dipole moment. This segmental mode is related to the dynamic glass transition of the bulk polymer. Furthermore, it is almost independent of molecular weight (Figure 1). In contrast the high temperature process exhibits a pronounced dependence on the molecular weight; it shifts to higher temperature with increasing molecular weight (Figure 1). This trend is characteristic for a normal-mode process, which corresponds to motions of the entire chain caused by dipole components parallel to the chain backbone. The empirical Williams–Landel–Ferry (WLF) equation[23] was used to describe the temperature dependence of the relaxation rate ν_{max} at maximum loss $\epsilon_{max}''(\nu)$

$$\log \frac{\nu_{max}}{\nu_0} = \frac{C_1(T - T_0)}{C_2 + T - T_0} \quad (1)$$

where T_0 is a reference temperature, ν_0 is the corresponding relaxation rate, and C_1 and C_2 are fitting parameters. The values of the parameters are calculated via nonlinear least-squares fits with $T_0 = 250$ K for the segmental-mode process and $T_0 = 300$ K for the normal-mode process. The results are listed in Tables III and IV. Attention is first directed to the segmental-mode process. For the linear *cis*-polyisoprene the relaxation rate and hence the activation parameters (Table III) are almost independent of molecular weight except for very low molecular weights. The same constants (Table IV) represent the experimental temperature dependence of the relaxation rate for the star polymers (Figure 4). From Tables III

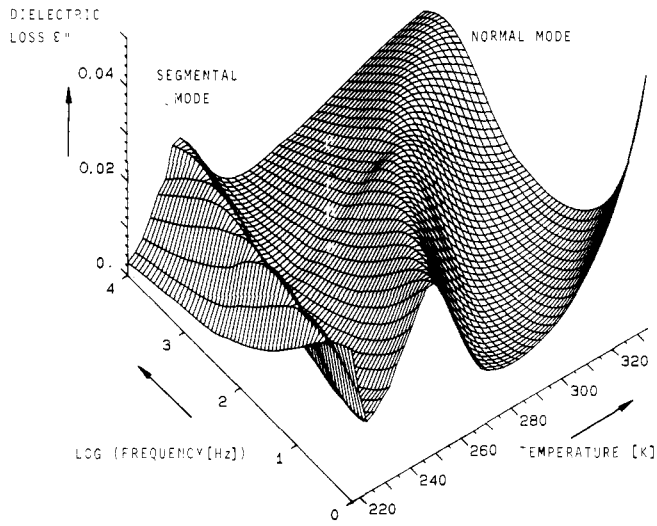

Figure 3. 3D representation of the frequency and temperature dependence of the dielectric loss, ϵ'', for the 18-arm polyisoprene star SPIP-18-11. (The steep rise at high temperatures and low frequencies is caused by the conductivity contribution to the dielectric loss.)

and IV it can be seen that the fractional free-volume values at $T_g(f_g/B = 1.2303C_1^g)$ are also unaffected by branching. The resulting values are in good agreement with those of synthetic rubber.[23] It thus appears clear that the segmental mode reflects a local mode of motion, independent of branching or chain length.[8]

The relaxation rates for normal-mode processes show a strong dependence on the molecular weight and demonstrate a weaker temperature dependence. The process in linear polymers and star polymers with nearly the same molecular weight or arm molecular weight (Figure 4) were compared, the following characteristics were observed:[1]

(i) Both polymer structures exhibit the same segmental-mode process.

(ii) The normal modes have a similar temperature dependence.

(iii) However, the normal modes of the star polymers are shifted to lower frequencies.

IV. Discussion

1. Dipole Geometry and Active Modes for the Normal-Mode Process. Linear flexible polymers having dipole moments aligned parallel to the chain contour (consistently head to tail) show a dielectric relaxation due to reorientation of the end-to-end vector. The resultant vector has been analyzed using the normal-mode description, and dielectric activity resides mainly in the first normal mode.[7] For star-shaped polymers where the parallel dipole moments of the single arms are always directed from the branch point to the end of the arms, the active modes are the second normal modes as shown earlier by Stockmayer.[7,8] The ends of the arms must each move out of phase with the branch point.

2. Molecular Weight Dependence of the Normal-Mode Relaxation Time. The relaxation times of linear *cis*-polyisoprene chains and 3-, 4-, 8-, 12-, and 18-arm stars calculated by using the relaxation $\tau = 1/2\pi\nu_{max}$ at 320 K are plotted versus the molecular weight or the arm molecular weight in Figure 5. As reported recently,[2-6] for linear *cis*-polyisoprene having molecular weights below the critical molecular weight, M_c ($\cong 10^4$), the normal-mode relaxation time was proportional to $M^{2.0}$ in agreement with the Rouse theory.[24] This low molecular weight region is a nonentangled region but above M_c the relaxation time follows the power law with an exponent of 3.7 ± 0.1, which is characteristic for entangled polymers.[25,26] The dependence of the relaxation time on the arm molecular weight for the various star polymers is in quantitative agreement with the 3.7 power of M_w as deduced for entangled linear chains above M_c.

3. Application of Theoretical Models and Computer Simulation. Graessley pointed out that the equilibration time for the conformational fluctuations of a tethered chain would be four times that for a free linear chain of the same length.[13] In order to compare the arm relaxation time with the relaxation time of a free linear chain, the molecular weight dependence of the latter is fitted at 320 K. A slope of 3.7 is found,[6] and this power law is used to interpolate the relaxation time at a given arm molecular weight. The results (Table IV) are in good agreement with the concept[13] mentioned above. In order to understand the presented results the scaling ansatz of Daoud and Cotton is used to describe the static melt properties of star polymers.[12] For high concentrations, $c > c^*$ (=overlap concentration), where branches of different stars overlap, the star consists of three separate regimes: (i) a close-packed core region where the branches are extended; (ii) an intermediate regime where the polymer has a single star behavior; and (iii) an outer region where the branches behave as linear chains.

When the concentration goes to unity, the interpenetration of different branches increases and the region where the stars do not overlap reduces to the core. Daoud and Cotton predicted the total radius, r, of the star in melt to be

$$r \propto l(f^{1/2} + N^{1/2}) \tag{2}$$

where f is the number of branches and every branch has N statistical units of length l. Thus, the radius is very weakly influenced by the number of arms. The structure in the melt is made of cores immersed in large regions where the different branches overlap strongly and behave like linear chains. This scaling picture will be employed to study the dynamical behavior of entangled star-shaped polymers.

Ham[9] assumed as early as 1957 that the effects of entanglements in a bulk polymer are the same for branched and linear polymers of the same molecular weight. De Gennes attempted to examine the stochastic motion of highly entangled star-branched polymers.[27,28] It was argued that to diffuse a 3-branched star molecule in a network of infinitely long, fixed obstacles one would have to withdraw the end of one of its arms down its tube to the branch point and extend it in the direction of another one of the arms. Using this assumption, de Gennes calculated that the relaxation time of the molecules, τ_s, would depend on chain length as

$$\tau_s \propto \exp(aN) \tag{3}$$

where a is a constant and N is the total number of chain segments. Klein[29] presented several approaches describing the dynamical quantities of star polymers and considered the diffusion and relaxation mechanisms of entangled stars in terms of the arm-retraction process.

Very recently Grest et al. presented a molecular dynamics simulation of many arm star polymers ($6 < f < 50$) for dilute solutions.[14,15] The Daoud–Cotton scaling picture for solutions was used to identify three typical relaxation mechanisms, which were studied separately for large N and f.

Table III
WLF Parameters C_1, C_2, and ν_o Determined by Eq 1 for the Segmental- and Normal-Mode Process of Linear Polyisoprene

	segmental mode, T_o = 250 K				normal mode, T_o = 300 K			normal mode, T = 320 K
code	C_1	C_2, K	$10^{-5}\nu_o$, Hz	$10^2 f_g/B$	C_1	C_2, K	ν_o, Hz	$-\log \tau$, s[a]
PIP-01					4.0	151.6	$2.0 \cdot 10^6$	7.1
PIP-05	5.7	80.0	1.2	3.5	4.0	133.9	$3.1 \cdot 10^4$	5.8
PIP-08	5.7	70.0	2.1	3.4	4.3	136.2	$7.4 \cdot 10^3$	5.2
PIP-13	5.8	74.3	2.2	3.6	4.2	128.8	$1.3 \cdot 10^3$	4.5
PIP-17	6.1	70.9	1.4	3.4	4.4	129.5	$3.9 \cdot 10^2$	4.0
PIP-38	6.0	71.2	1.6	3.5	4.2	119.9	$2.2 \cdot 10^1$	2.7
PIP-65	6.1	73.4	1.7	3.5	3.6	97.5	3.1	1.9
PIP-97	6.1	70.9	1.4	3.4	0.9	57.9	0.02	1.1

[a] The normal-mode relaxation time, τ, is obtained from $\tau = (2\pi\nu_{max})^{-1}$.

Table IV
WLF Parameters C_1, C_2, and ν_o Determined by Eq 1 for the Segmental- and Normal-Mode Process of Multiarmed Polyisoprene Stars

	segmental mode, T_o = 250 K				normal mode, T_o = 300 K			normal mode, T = 320 K	
code	C_1	C_2, K	$10^{-5}\nu_o$, Hz	$10^2 f_g/B$	C_1	C_2, K	ν_o, Hz	$-\log \tau$, s[a]	$-\log \tau_{tethered}$, s[b]
SPIP-3-11	6.2	75.4	1.6	3.6	3.7	111.8	3.4×10^2	3.9	4.0
SPIP-4-15	6.3	76.7	1.3	3.6	3.9	116.6	2.4×10^2	3.6	3.5
SPIP-4-30	6.2	78.7	1.3	3.6	2.3	40.0	1.6		
SPIP-4-44	6.2	79.4	1.3	3.8					
SPIP-4-95	6.3	74.9	1.4	3.5					
SPIP-8-05	6.0	75.2	1.5	3.6	4.3	132.8	9.6×10^3	5.3	5.1
SPIP-8-08	6.0	72.5	1.1	3.6	4.2	127.5	2.2×10^3	4.7	4.7
SPIP-8-14	6.1	76.7	1.5	3.6	4.1	123.3	1.6×10^2	3.5	3.5
SPIP-8-16	6.3	76.6	1.4	3.6	4.0	122.4	1.3×10^2	3.7	3.7
SPIP-8-100	6.0	76.3	1.5	3.8					
SPIP-12-03	6.0	79.6	2.0	3.7	4.2	134.7	9.1×10^3	5.4	5.4
SPIP-12-08	6.1	79.8	2.0	3.7	4.0	128.8	1.8×10^3	4.6	4.7
SPIP-12-21	5.9	76.7	1.9	3.8	3.4	104.3	5.3×10^3	3.1	3.0
SPIP-12-68	6.2	73.8	1.0	3.5					
SPIP-18-03	6.3	74.9	1.3	3.5	4.7	140.8	3.1×10^4	5.7	5.4
SPIP-18-11	6.1	72.1	1.3	3.5	3.8	115.0	5.5×10^2	4.1	4.1
SPIP-18-12	6.0	72.6	1.5	3.5	3.8	114.3	3.1×10^2	3.8	3.9
SPIP-18-21	6.2	75.0	1.3	3.5	3.4	100.4	5.4×10^1	3.1	3.1
SPIP-18-44	6.2	75.1	1.3	3.5					

[a] The normal-mode relaxation time, τ, is obtained from $\tau = (2\pi\nu_{max})^{-1}$. [b] The relaxation time of a tethered chain is calculated by $\tau_{tethered} = 4\tau_{linear}$, where τ_{linear} is the relaxation time for a free chain of the same length.

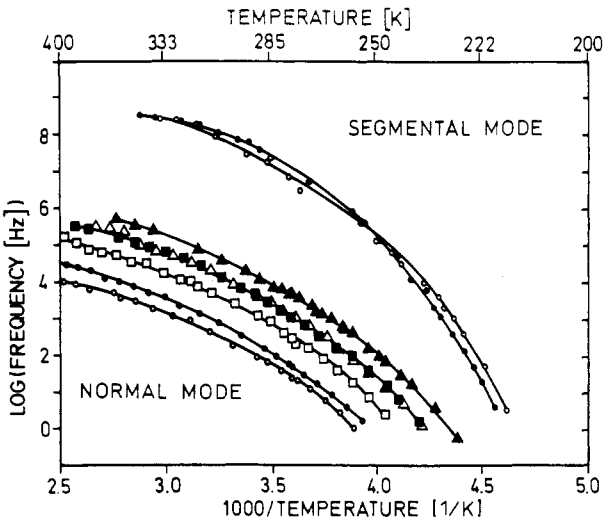

Figure 4. Activation plot for the segmental mode and normal mode of the 8-arm polyisoprene star and the linear *cis*-polyisoprene (for the sake of clarity the segmental modes for SPIP-8-14 and PIP-13 are plotted only): △, SPIP-8-05; ▲, PIP-05; □, SPIP-8-08; ■, PIP-08; ○, SPIP-8-14; ●, PIP-13.

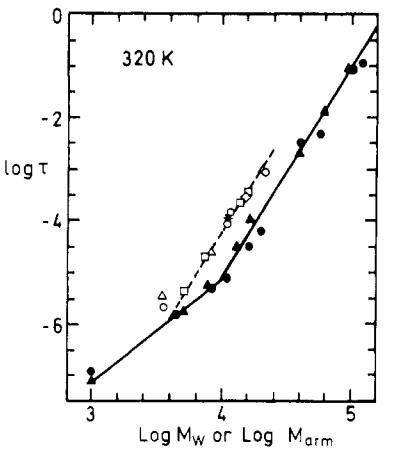

Figure 5. Dependence of dielectric relaxation time, τ, on molecular weight for the normal mode of the linear polyisoprene chain (▲) at 320 K, data reported by Adachi and Kotaka (●)[2,3] and of the star-branched polyisoprene: *, 3-arm star; ◇, 4-arm star; □, 8-arm star; △, 12-arm star; ○, 18-arm star.

The first describes elastic deformation of the star's overall shape and is essentially independent of the number of arms, f. The longest relaxation time for the free-draining (Rouse) case scales with

$$\tau_s \propto N^{1+2\nu} f^{1-[(1+2\nu)/2]} = N^{2.18} f^{-0.09} \quad (4)$$

where $\nu = 0.59$ for a good solvent ($d = 3$). This result supports the scaling picture where the shape relaxation depends imperceptibly on f compared to the independent strand approach of Zimm and Kilb,[10] which pre-

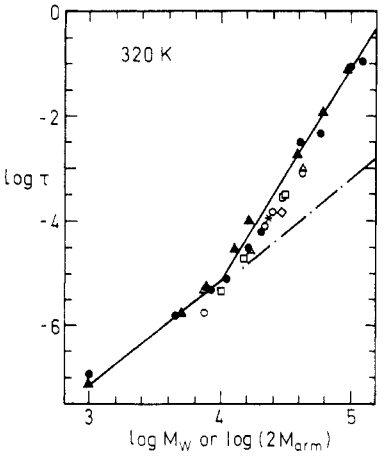

Figure 6. Dependence of dielectric relaxation time, τ, on molecular weight, M_w, for the normal mode of the linear polyisoprene chain (▲) at 320 K, data reported by Adachi and Kotaka (●).[2,3] For the star-branched polyisoprene, the dielectric relaxation time is plotted versus $2M_{arm}$: *, 3-arm star; ◇, 4-arm star; □, 8-arm star; △, 12-arm star; ○, 18-arm star. (The dot-dash line represents the maximum relaxation time, τ_R, in the Rouse theory.[24])

dicts $\tau_s \sim f$. The intermediate relaxation process occurs via rotational diffusion, which is slower since it is not enhanced by the pressure within the star, as the elastic modes are. Both relaxation processes scale the same with molecular weight of their arms as for linear polymers, but they show different dependences on the number of arms. A third relaxation process is the disentanglement of two or more arms. For a star polymer it is predicted that this relaxation time depends exponentially on $f^{1/2}$.

When the scaling ansatz of Daoud and Cotton[12] and the results of the computer simulation of Grest et al. are combined,[14] the dielectric normal-mode relaxation can be explained as follows. For the shape relaxation of the entangled star second normal modes have to propagate over a distance of the order of the diameter R of the star polymer. Therefore, a span molecular weight for a star $M_{span} = 2M_{arm}$ is introduced in order to cover the extended size of the star. Accordingly, the relaxation time for this process corresponds to the correlation time for the end-to-end distance $\langle R(0)\, R(t)\rangle$.

As deduced by Grest et al.[15] for dilute solutions the relaxation times of the end-to-end distance R depend imperceptibly on f. The influence of the arms on each other in the undiluted entangled state is assumed to vary not greatly with the number of arms.[30] The experimental results for the different molecular architectures are shown in Figure 6 where log τ is plotted against log ($2M_{arm}$) for the stars and against log M_w for the linear polymers. The data support the scaling picture (eq 2) that in the undiluted state single star behavior is reduced to the core and star-branched polymers behave like linear chains within the studied molecular weight range. For samples having a span molecular weight below the critical molecular weight, M_c (e.g., SPIP-12-03 and SPIP-18-03), a restiction has to be made. When the branches are not very long, the single star region is extended and one has to define an effective concentration, $\bar{c}$, in the overlapping regions as earlier proposed by Daoud and Cotton.

V. Conclusion

We have studied the dielectric relaxation behavior of multiarmed *cis*-polyisoprene stars as well as linear *cis*-polyisoprene in the bulk amorphous state. The molecular weight dependence of the normal-mode relaxation time for linear polymers below a critical molecular weight, M_c ($\cong 10^4$), obeys the Rouse theory, where τ is proportional to $M^{2.0}$. Above M_c the relaxation time is proportional to $M^{3.7}$, which is characteristic for reptational motions.

The segmental-mode process for both linear and star-branched *cis*-polyisoprene is found to be almost independent of molecular weight and hence results in similar activation parameters. This process is directly associated with the dynamic glass transition of the bulk polymer.

The arm relaxation time can be compared in good agreement with the conformational relaxation time of a tethered chain as deduced by Graessley. The dependence of the relaxation time on the span molecular weight ($=2M_{arm}$) for multiarmed star polymers is in quantitative agreement with the 3.7 power as deduced for linear chains above M_c. This course is explained with the conformational scaling properties of Daoud and Cotton and computational molecular dynamics simulation. The latter reveals a relaxation mechanism where the star relaxes via overall shape fluctuation, which has a radial dimension of the order of span molecular weight. The corresponding relaxation times depend imperceptibly on the number of arms. The scaling ansatz predicted for the end–center distance has a similar dependence. The single star behavior is reduced to the close-packed core region, but for distances larger than this region the different branches interpenetrate strongly and behave like linear chains.

Acknowledgment. D.B. is grateful to Prof. E. W. Fischer, Dr. K. Kremer, and A. Zetsche for helpful discussions.

References and Notes

(1) Boese, D.; Kremer, F.; Fetters, L. J. *Makromol. Chem., Rapid Commun.* **1988**, *9*, 367.
(2) Adachi, K.; Kotaka, T. *Macromolecules* **1984**, *17*, 120.
(3) Adachi, K.; Kotaka, T. *Macromolecules* **1985**, *18*, 466.
(4) Adachi, K.; Kotaka, T. *J. Mol. Liq.* **1987**, *36*, 75.
(5) Imasishi, Y.; Adachi, K.; Kotaka, T. *J. Chem. Phys.* **1988**, *89*, 7585.
(6) Boese, D.; Kremer, F., submitted for publication in *Macromolecules*.
(7) Stockmayer, W. H. *Pure Appl. Chem.* **1967**, *15*, 539.
(8) Stockmayer, W. H.; Burke, J. J. *Macromolecules* **1969**, *2*, 647.
(9) Ham, J. S. *J. Chem. Phys.* **1957**, *26*, 625.
(10) Zimm, B. H.; Kilb, R. W. *J. Polym. Sci.* **1957**, *37*, 19.
(11) Adachi, K.; Kotaka, T. *Macromolecules* **1983**, *16*, 1936.
(12) Daoud, M.; Cotton, J. P. *J. Phys. (Paris)* **1982**, *43*, 531.
(13) Graessley, W. W. *Adv. Polym. Sci.* **1982**, *47*, 67.
(14) Grest, G. S.; Kremer, K.; Witten, T. A. *Macromolecules* **1987**, *20*, 1376.
(15) Grest, G. S.; Kremer, K.; Milner, S. T.; Witten, T. A. *Macromolecules* **1989**, *22*, 1904.
(16) Morton, M.; Fetters, L. J. *Rubber Chem. Technol.* **1975**, *48*, 359.
(17) Hadjichristidis, N.; Guyot, A.; Fetters, L. J. *Macromolecules* **1978**, *11*, 668.
(18) Hadjichristidis, N.; Fetters, L. J. *Macromolecules* **1980**, *13*, 191.
(19) Kow, C.; Morton, M.; Fetters, L. J.; Hadjichristidis, N. *Rubber Chem. Technol.* **1982**, *55*, 245.
(20) Bauer, B. J.; Fetters, L. J.; Graessley, W. W.; Hadjichristidis, N.; Quack, G. F. *Macromolecules* **1989**, *22*, 2237.
(21) Sato, H.; Ono, A.; Tanaka, Y. *Polymer* **1977**, *18*, 580.
(22) Pugh, J.; Ryan, J. T. *IEEE Conf. Dielectr. Mater., Meas. Appl.* **1979**, 144, 404.
(23) Ferry, J. D. *Viscoelastic Properties of Polymers*, 3rd ed.; Wiley: New York, 1980.
(24) Rouse, P. E. *J. Chem. Phys.* **1953**, *21*, 1272.
(25) de Gennes, P.-G. *J. Chem. Phys.* **1971**, *55*, 572.
(26) Doi, M.; Edwards, S. F. *J. Chem. Soc., Faraday Trans. 2* **1978**, *74*, 1789, 1802, 1818.
(27) de Gennes, P.-G. *J. Phys. (Paris)* **1975**, *36*, 1199.
(28) de Gennes, P.-G. *Scaling Concepts in Polymer Physics*; Cornell University Press: New York, 1979.
(29) Klein, J. *Macromolecules* **1986**, *19*, 105.
(30) Stockmayer, W. H., private communication.